Research Square

Preprints are preliminary reports that have not undergone peer review.
They should not be considered conclusive, used to inform clinical practice,
or referenced by the media as validated information.

Promotion of wound healing by insulin-like growth factor-1-loaded Bombyx mori L. silk fibroin films in diabetic mice

Meng-Jin Lin
Miaoli District Agricultural Research and Extension Station, Council of Agriculture, Executive Yuan
Mei-Chun Lu
Miaoli District Agricultural Research and Extension Station, Council of Agriculture, Executive Yuan
Yun-Chen Chan
Miaoli District Agricultural Research and Extension Station, Council of Agriculture, Executive Yuan
Hwan-You Chang (hychang@life.nthu.edu.tw)
National Tsing Hua University

Research Article

Keywords: Wound-dressing, Degumming Process, Cell Growth Promotion, Wound Closure, Diabetic Wounds

Posted Date: April 12th, 2021

DOI: https://doi.org/10.21203/rs.3.rs-400183/v1

License: This work is licensed under a Creative Commons Attribution 4.0 International License.
Read Full License

Abstract

This study aimed to engineer an advanced wound-dressing combining *Bombyx mori* L. silk fibroin (SF) with insulin-like growth factor-1 (IGF-1). Silk fibroin was purified through a newly-developed high-temperature degumming process and cast on a hydrophobic surface to form SF-films. The process allowed the fabrication of a film exhibiting a 42% increase in transparency and a 32% higher proliferation rate of BALB/3T3 fibroblasts compared to that obtained by conventional alkaline treatment. This study demonstrated that the optimal concentration of IGF-1 to promote BALB/3T3 cell growth in hyperglycemic medium was approximately 130 nM. Further analysis of wound healing in a diabetic mouse model indicated that SF-film loaded with 3.25 pmol IGF-1 showed significantly superior wound closure (13% increase) at 13 days after treatment compared to treatment with 65 pmol free IGF-1. We clearly observed improvement in diabetic wound healing exerted synergistically by SF-film and IGF-1, as reflected by parameters including degree of re-epithelialization, epithelial tissue area, and angiogenesis. These results strongly suggest the great potential of IGF-1-loaded SF-film as a dressing for the treatment of diabetic wounds.

Introduction

Diabetes mellitus is one of the most prevalent non-communicable diseases, affecting 422 million adults in 2014 and causing about 1.5 million deaths in 2012[1]. Approximately 15% of diabetic patients suffer from chronic wounds that frequently lead to limb amputation or even death[2,3]. In 2010, approximately 73,000 amputations were performed on diabetic patients with non-healing wounds in the United States[4]. Although significant efforts have been exerted to improve diabetic wound healing, no satisfactory therapy has been developed thus far[5]. Therefore, more research on novel interventions to improve healing of diabetes-associated chronic wounds is urgently required.

Compared to wounds caused by trauma or burn, chronic diabetic wounds show a higher degree of aberrant angiogenesis, and lack of essential growth factors such as insulin-like growth factors (IGFs) [6,7]. An early report has demonstrated that the distribution of IGF-1 is restricted to the stratum granulosum and spinosum of uninjured skin and is absent at the edge of diabetic foot ulcers, suggesting its importance in healing chronic diabetic wounds [8]. IGF-1 is a 7.6-kDa single-chain polypeptide with three intramolecular disulfide bridges. The IGF-1 receptor is a transmembrane receptor tyrosine kinase that exhibits auto-phosphorylation activity when activated by IGF-1[9]. Activation of the IGF-1 receptor results in phosphorylation of insulin receptor substrates and Shc, thus, initiating the cell proliferation pathway[10]. IGF-1 stimulates the Akt signaling pathway and promotes corneal epithelial cell growth for eye wound healing [11,12]. Although IGF-1 is a potential candidate for the treatment of wound healing [13], the critical dosage and short half-life of IGF-1 (< 15 min) limits its application [14,15]. Therefore, development of a delivery system to maintain the activity of IGF-1 is necessary for clinical therapy.

Silk fibroin from the common silkworm *Bombyx mori* L. is a biomaterial with excellent mechanical strength, biocompatibility, biodegradability, and immunogenicity [16-18]. Silk fibroin is secreted from the posterior silk gland as a 2.3-MDa elementary unit, consisting of six sets of a disulfide-linked 350-kDa heavy chain/24–26-kDa light chain heterodimer and one molecule of fibrohexamerin/P25 [19]. *B. mori* fibroin is mainly composed of glycine (43%), alanine (30%), and serine (12%) [20]. Silk fibroin could form a sustained drug delivery platform though specious modification[21]. Previous studies also indicated that silk fibroin not only has strong stimulatory effects on cell attachment and proliferation [22-24], but also inhibits wound scar formation in excisional or burn wounds [25,26]. The protein has been tested in several modalities, including film [27-29], sponge [30], hydrogel [31], and electrospun mat [32-34]. Nevertheless, little is known about the effect of different silk fibroin manufacturing procedures on wound healing. In addition, although silk fibroin may be an excellent carrier of IGF-1 for wound healing, the most effective form of combining silk fibroin and IGF-1 has never been explored.

Therefore, the aim of this study was to engineer an advanced wound-dressing combining silk fibroin with IGF-1. The dosage-effect of IGF-1, and how it affects the efficiency of silk fibroin/IGF-1 were investigated in this study. Further, we characterized the effect of exogenous IGF-1 conjugated with the fibroin film on wound healing *in vivo* to develop a better therapy for diabetic wound healing.

Results

Manufacturing procedure of silk fibroin (SF)-film

Removal of sericin via degumming is a critical step in the production of biocompatible fibroin preparations for wound healing treatment. This study compared the properties of SF-films prepared with new fibroin film production procedure via conventional alkaline degumming (AD) or the experimental heating degumming (HD). The average weight loss of silk during AD treatment was 31.4%, which was higher than that of HD treatment (29.5–29.8%) irrespective of the treatment period (Figure 2a). However, the thickness of SF-films produced by the two procedures was approximately the same (56–62 μm) (Figure 2b). Film transparency, an indicator of fibroin purity, was 42% higher in the HD group than in the AD group ($p < 0.001$) (Figure 2c). The proliferation rate of BALB/3T3 fibroblasts grown on HD-derived SF-film was higher than that of cells grown on AD-derived film by 14%–32% (Figure 2d). In SDS-PAGE electrophoresis, the accumulation of light chain fibroin protein (about 24–26kDa) was higher in the HD group than in the AD group (Figure 2e).

Effect of different concentrations of IGF-1 on cell migration

To identify the optimal concentration of IGF-1 for use on diabetic wounds, we investigated the effect of different concentrations of IGF-1 on migration, cytotoxicity, and proliferation of BALB/3T3 fibroblasts following 144-h exposure. The closure rates of artificially created gaps in BALB/3T3 monolayers after treatment with different IGF-1 concentrations (65 to 520 nM) for five days were determined. The addition of IGF-1 up to 260 nM in the hyperglycemic medium (50 mM glucose) clearly promoted cell migration.

The optimal concentration of IGF-1 was around 130 nM, which enhanced cell migration rate by 23% after 96 h. Higher concentrations of IGF-1 inhibited cell migration. At 520 nM IGF-1, the migration rate of BALB/3T3 fibroblasts decreased significantly (17.6%, $p < 0.001$) after 96 h (Figure 3a, b) compared to the control. No significant difference was observed in BALB/3T3 cell cytotoxicity and proliferation between any of the tested IGF-1 concentrations (Figure 3c, d).

Effect of SF-film loaded with IGF-1 (SF-film–IGF-1) on wound healing of BALB/3T3 monolayers

We compared the effects of IGF-1 alone, SF-film, and SF-film–IGF-1 on wound closure and proliferation of BALB/3T3 fibroblasts in regular and hyperglycemic medium. In regular culture medium, there was no significant difference in the wound healing of BALB/3T3 cells between any of the treatments (Figure 4a). In contrast, wound closure was enhanced by approximately 16% in the presence of 130 nM free IGF-1 cultured for 48 h in hyperglycemic medium. The enhancement of wound closure in hyperglycemic conditions was especially evident in the presence of IGF-1 and SF-film–IGF-1, with more than 30% acceleration after treatment for 96 h (Figure 4b).

In vivo wound healing studies of SF-film–IGF-1

We investigated whether SF-film–IGF-1 promotes wound healing in diabetic mice. A mouse line deficient in leptin receptor, and exhibiting several hallmarks of diabetes including hyperglycemia, obesity, and impaired wound healing, was used in this study. As shown in Figure 5a, the wound closure in the experimental groups (IGF-1, SF-film, and SF-film–IGF-1) was significantly faster than that in the PBS-treated controls. Callus formation and micro-vessel accumulation could be observed as early as three and five days post-treatment, respectively, in the SF-film treatment group (Figure 5b). The wound area of *db/db* mice treated with 3.25 pmol IGF-1 either in solution or complexed with SF-film recovered by about 20% on day 6, and the wounds healed 25.3% and 19.2%, respectively, after treatment for eight days. The improvement in the SF–film-IGF-1 group continued and resulted in a 12.8% smaller wound area than that in the control group on day 13 (Figure 5c). However, an increase in IGF-1 dose did not yield a better outcome. Thus, we concluded that among all experimental groups, SF-film–IGF-1 with a relatively low dose of IGF-1 is optimal for the treatment of diabetic wounds (Figure 5d).

Histology of regenerated tissue in SF-film-treated diabetic wounds

We examined wound histology by Masson's trichrome staining (Figure 6). The wound edge was defined as the longest distance between the two boundaries of intact skin. Wound-edge distances of SF-film treated groups, with or without IGF-1, were significantly shorter than those in other groups, demonstrating the ability of SF-film to promote wound healing (Figure 7a). We further analyzed the epithelial gap and re-epithelialization of the regenerated tissue to assess the status of wound closure. SF-film loaded with either low (3.25 pmol) or high (65 pmol) doses of IGF-1 resulted in a smaller epithelial gap and better re-epithelialization (Figure 7b, d). In particular, the epithelial tissue area of the wound treated with SF-film loaded with 3.25 pmol IGF-1 increased significantly ($p < 0.05$) compared with that of the control group (Figure 7c). Because the presence of blood vessels is an important measure of dermal restoration, we

investigated the expression of CD31, an endothelial cell-specific marker, in different experimentally treated wounds. SF-film treatment seemed to enhance angiogenesis (Figure 8). These results indicate that SF-film loaded with a low dosage of IGF-1 is a useful dressing for diabetic wound treatment.

Discussion

Raw silk fibers comprise primarily two protein components, fibroin and sericin. Sericin constitutes approximately 25–30% (w/w) of the silkworm cocoon[20]. Because of its high immunogenicity, sericin must be removed through degumming before the silk can be used in the human body. The degumming reagents, treatment time, and temperature are key factors that can affect sericin removal[35]. In this study, we have established a novel SF production method with modifications to degumming, dialysis, and purification procedures to improve SF purity and hence the biocompatibility of the SF-film. Although the weight loss of silk fiber after degumming using the AD method was not significantly different from that achieved when using the HD method (29.5% vs. 31.4%), the transparency of the films and proliferation of cells grown on the films were quite distinct. A higher purity of SF, as reflected by the transparency of SF-film and accumulation of fibroin L-chain protein, was achieved using the HD procedure. Further, we observed better cell growth of fibroblasts on the fibroin film produced via the new production method. An SF-film of a high purity is advantageous in its ability to support cell proliferation, as demonstrated in this study, and may also reduce allergic reaction when used in vivo [36,37]. Our finding is consistent with previous studies where a higher purity of SF could be obtained by heating under pressure compared to treatment with sodium carbonate solution [38,39]. Another advantage of using HD over AD in SF manufacturing is that HD is less time consuming and uses significantly less reagents and water. Together, these findings strongly suggest that our new fibroin film production method with HD is superior to traditional methods.

IGF-1 is an important hormone produced by the liver that regulates secretion and physiological activities of growth hormone [40-42]. Among the activities associated with IGF-1 are stimulation of the proliferation and migration of vascular smooth muscle cells and keratinocytes [43-46]. To apply IGF-1 and IGF-1 loaded SF-film in diabetic wound treatment, we first determined the optimal IGF-1 dosage for effective wound healing in both cultured cells and diabetic animals. In regular glucose conditions, there was no significant difference in the migration rate of cells grown in free IGF-1 and those grown on SF-film loaded with different concentrations of IGF-1. In contrast, when testing BALB/3T3 fibroblasts grown in hyperglycemic medium, cell migration was enhanced at lower IGF-1 concentrations (65–260 nM), while higher IGF-1 concentrations (520 nM) had an inhibitory effect. Interestingly, proliferation of BALB/3T3 cells was not stimulated by 65–520 nM IGF-1. Similar results were also observed in a previous study, which showed that IGF-1 functions primarily to increase the cell sizes rather than proliferation rates of chondrocytes [47]. These results suggest that, in the cell gap repair assay under hyperglycemic conditions, IGF-1 functions in a dose-dependent fashion to enhance BALB/3T3 cell migration, with saturation at 260–520 nM .

Similar to the results found in cultured cells, wound repair in diabetic mice was accelerated at a low dose of IGF-1 (3.25 pmol), while it was inhibited at a high dose (65.0 pmol). Although treatment with IGF-1 alone also produced a good wound area reduction after six days, only SF-film–IGF-1 significantly decreased the wound size at later stages of repair. Additional wound healing parameters, including the epithelial gap distance, re-epithelialization degree, and epithelial tissue area, were significantly improved in the SF-film–IGF-1 group compared with the IGF-1 alone group. This finding is supported by an earlier study which demonstrated that IGF-1 alone only promoted the growth of myofibroblasts, but not tissue vascularization [48]. Interestingly, SF-films in the absence of IGF-1 also showed accelerated callus and micro-vessel formation in wounds of *db/db* mice. Both inflammation and wound edges were markedly reduced, while angiogenesis was enhanced in the SF-film treated wounds irrespective of IGF-1 presence. The SF-film is likely to assist wound healing through the enhancement of fibroblast migration and blood vessel tube growth, although the mechanism behind this phenomenon remains unclear and requires further investigation.

Compared with free IGF-1 treatment, SF-film-IGF-1 showed better effects, regardless of the amount of loaded IGF-1. There were no significant differences in wound area, wound edge, epithelial gap, or re-epithelialization in diabetic wounds treated with SF-film loaded with two different IGF-1 doses. This was likely due to sustained release of IGF-1 from the SF-films. These results strongly suggest that SF-film serves as a reservoir for slow release of IGF-1 and that consistent levels of the growth factor are beneficial to diabetic wound healing.

As far as we are aware, this study is the first to evaluate SF-film as an IGF-1 carrier in diabetic wound repair. Our results demonstrated that SF-film plays dual roles as a wound healing dressing and IGF-1 delivery scaffold. SF-film carrying a low dosage of IGF-1 is an ideal wound dressing and may find real application in diabetes-associated wound treatment.

Materials & Methods

Preparation of SF films

Silkworms were reared with mulberry leaves at 28 °C in our specifically designated facility (Taiwan Silkworm Germplasm, Miaoli District Agricultural Research and Extension Station, Taiwan). Cocoons were harvested, washed, and then degummed using previously described procedures [17,18] by boiling in 0.02 M sodium carbonate solution (alkaline degumming, AD). Alternatively, cocoons were heated in deionized water (1% w/v) at 1.2 kg/cm^2 pressure for 1, 2, and 3 h (heating degumming, HD) to remove sericin from raw silk. The SF fibers were dried at 50 °C for 24 h. The weight loss was determined using the formula, $W_L = [(W_0-W_1)/W_0] \times 100\%$, where W_L is the percentage weight loss, W_0 is the initial weight of the cocoon (mg), and W_1 is the final weight of dry SF fibers (mg). Dry SF fibers were dissolved in 9.3 M lithium bromide solution (20% w/v) at 60 °C for 6 h and dialyzed against deionized water. The final concentration of fibroin in the aqueous silk solution was adjusted to 2 g/L as determined by the Bradford protein assay (Thermo Fisher Scientific, Waltham, MA, USA). The turbidity of the silk fibroin aqueous solution was

measured at 660 nm using a spectrophotometer (Infinite M2000pro, TECAN, Switzerland). The solution was cast on polydimethylsiloxane (PDMS) substrates and allowed to dry and form an SF-film. The films were water vapor annealed by subjecting them to a water vapor environment in an air-evacuated desiccator to increase the ratio of beta-sheet crystallinity and hence mechanical strength. The SF-films were sterilized with 70% ethanol and UV-irradiation, soaked in different concentrations of IGF-1 (SRP3069, Sigma-Aldrich, St Louis, MO, USA) for 48 h at 4 °C, and washed in phosphate-buffered saline (PBS, pH 7.4) for 12 h at 4 °C. The standard procedure for producing IGF-1 loaded SF-films is illustrated in Figure 1.

Sodium dodecyl sulfate-polyacrylamide gel electrophoresis (SDS-PAGE)

Briefly, ten microliters of the degummed protein samples along with pre-stained protein ladder (BioMan Laboratories, Taiwan) was subjected to SDS-PAGE analysis at a constant 150 V. Gels were subsequently stained with InstantBlue commassie protein stain (Merck, Germany) for 12 h at room temperature, and gel images were captured with an iBright FL1000 Image system (Thermo Fisher Scientific, Waltham, MA, USA).

BALB/3T3 migration, viability, and proliferation studies

Mouse BALB/3T3 fibroblasts were cultured in Dulbecco's Modified Eagle's Medium (DMEM) supplemented with 25 mM D-glucose and 10% fetal bovine serum under 5% CO_2 at 37 °C. The cells were seeded into a 24-well plate at 1 × 10^6 cells/well in the presence of a CytoSelect™ Wound Healing Insert (Cell Biolabs, San Diego, CA, USA). After incubating for 12 h, the insert was removed carefully to create a 500-μm-width cell gap. The cells were treated with SF-film, IGF-1, or SF-film–IGF-1 in medium containing either 25 mM (regular medium) or 50 mM (hyperglycemic medium) D-glucose. Wound closure was serially imaged at different times (0, 3, 6, 8, 10, and 13 days) post scratching using an inverted light microscope (ECLIPSE Ts2-FL, Nikon, Japan).

Cell viability after treatment for three days was measured with the LIVE/DEAD™ Viability/Cytotoxicity Kit (Thermo Fisher Scientific, Waltham, MA, USA) and examined under a fluorescence microscope according to the manufacturer's instruction. For the cell proliferation assay, cells were incubated with 10% alamarBlue assay reagent (Thermo Fisher Scientific, Waltham, MA, USA) in DMEM for 4 h under 5% CO_2 at 37 °C. The fluorescence of the culture supernatant was determined with excitation and emission wavelengths of 570 and 600 nm, respectively. The cell proliferation rate was calculated according to the formula provided by the dye manufacturer.

In vivo wound-healing studies

The murine diabetic wound healing assay was conducted in the animal facility following the ARRIVE guidelines approved by the Institutional Animal Care and Use Committee of the National Taiwan University and conducted according to the NIH Guide for the Care and Use of Laboratory Animals. Six-week-old leptin-receptor deficient BKS.Cg-*Dock7*$^{m\ +/+}$ *Lepr*^{db}/ JNarl female mice (*db/db*) were purchased from the National Laboratory Animal Center (Taiwan) and acclimatized in the animal facility for one

week. Mice were housed in polycarbonate shoebox cages with hardwood bedding at 21 ± 1 °C with a 12 h/12 h light/dark cycle and had free access to water and food. Before wound induction, the plasma glucose levels of the mice were confirmed to be above 300 mg/dL to ensure their hyperglycemic state. After anaesthetization with isoflurane, middorsal full-thickness wounds, 8 mm in diameter including epidermis and dermis, were created. Mice were divided into the following treatment groups: A, PBS (control group); B, 3.25pmol IGF-1 (low IGF-1 group); C, 65pmol IGF-1 (high IGF-1 group); D, a circular SF-film (10-mm in diameter); E, a circular SF-film containing 3.25 pmol IGF-1 (SF-film-low IGF-1 group); and F, a circular SF-film containing 65 pmol IGF-1 (SF-film-high IGF-1 group). All treatments were applied to the wound beds directly and covered with a sterile adhesive film to maintain a moist environment. Wound healing was examined and recorded every 2–3 days using a digital camera at the same distance with a calibration scale on the side.

Histological and immunohistochemical analyses

Wound tissues were harvested from the sacrificed animals at the indicated time points, fixed in formalin overnight, and then embedded in paraffin. The fixed tissues were then sliced into 5-μm sections and stained using Masson trichrome stain kit (StatLab, Lodi, CA, USA) for histological analysis. Sections were then deparaffinized, rehydrated, and subjected to sodium citrate buffer antigen retrieval. Sections were then stained with CD31 antibody (Genetex, Irvine, CA, USA) at 1:100 dilution using an automated immunohistochemistry system (BOND-MAX, Leica, Germany) and visualized under a light microscope (IM-3, OPTIKA, Italy).

Statistical analyses

All data are presented as mean ± SEM for each group. Multiple comparisons were evaluated by one-way analysis of variance (ANOVA) followed by Dunnett's multiple comparison post hoc test to assess statistically significant differences (*$p < 0.05$, **$p < 0.01$, and ***$p < 0.001$) between control and experimental samples. Analyses were performed using SAS-EG 7.1 software (SAS Enterprise Guide, SAS Institute Inc.). All error bars represent the standard error of the mean (SEM).

Declarations

Acknowledgments

The Council of Agriculture, Executive Yuan, Republic of China (Taiwan), supported this study.

References

1 WHO. *Global report on diabetes*. (2016).

2 Lamers, M. L., Almeida, M. E., Vicente-Manzanares, M., Horwitz, A. F. & Santos, M. F. High glucose-mediated oxidative stress impairs cell migration. *PLoS One* **6**, e22865, doi:10.1371/journal.pone.0022865

(2011).

3 Yach, D., Stuckler, D. & Brownell, K. D. Epidemiologic and economic consequences of the global epidemics of obesity and diabetes. *Nat. Med.* **12**, 62–67 (2006).

4 Randeria, P. S. *et al.* siRNA-based spherical nucleic acids reverse impaired wound healing in diabetic mice by ganglioside GM3 synthase knockdown. *Proc. Natl. Acad. Sci. USA* **112**, 5573–5578, doi:10.1073/pnas.1505951112 (2015).

5 Ram, M. *et al.* Bilirubin modulated cytokines, growth factors and angiogenesis to improve cutaneous wound healing process in diabetic rats. *Int Immunopharmacol* **30**, 137-149, doi:10.1016/j.intimp.2015.11.037 (2016).

6 Li, J., Zhang, Y. P. & Kirsner, R. S. Angiogenesis in wound repair: angiogenic growth factors and the extracellular matrix. *Microsc Res Tech* **60**, 107-114, doi:10.1002/jemt.10249 (2003).

7 Soneja, A., Drews, M. & Malinski, T. Role of nitric oxide, nitroxidative and oxidative stress in wound healing. *Pharmacol. Rep.* **57 (suppl.)**, 108–119 (2005).

8 Blakytny, R., Jude, E. B., Gibson, J. M., Boulton, A. J. M. & Ferguson, M. W. J. Lack of insulin-like growth factor 1 (IGF1) in the basal keratinocyte layer of diabetic skin and diabetic foot ulcers. *J. Pathol.* **190**, 589–594 (2000).

9 Wu, Y. C., Zhu, M. & Robertson, D. M. Novel nuclear localization and potential function of insulin-like growth factor-1 receptor/insulin receptor hybrid in corneal epithelial cells. *PLoS One* **7**, e42483, doi:10.1371/journal.pone.0042483 (2012).

10 Jung, H. J. & Suh, Y. Regulation of IGF -1 signaling by microRNAs. *Front. Genet.* **5**, 1–13, doi:10.3389/fgene.2014.00472 (2015).

11 Nagano, T. *et al.* Effects of substance P and IGF-1 in corneal epithelial barrier function and wound healing in a rat model of neurotrophic keratopathy. *Invest. Ophthalmol. Vis. Sci.* **44**, 3810–3815, doi:10.1167/iovs.03-0189 (2003).

12 Stuard, W. L., Titone, R. & Robertson, D. M. The IGF/insulin-IGFBP axis in corneal development, wound healing, and disease. *Front. Endocrinol. (Lausanne)* **11**, 1–15, doi:10.3389/fendo.2020.00024 (2020).

13 Blakytny, R., Jude, E. B., Gibson, J. M., Boulton, A. J. M. & Ferguson, M. W. J. Lack of insulin-like growth factor 1 (IGF1) in the basal keratinocyte layer of diabetic skin and diabetic foot ulcers. *J Pathol.* **190**, 589-594 (2000).

14 Guler, H. P., Zapf, J., Schmid, C. & Froesch, E. R. Insulin-like growth factors I and II in healthy man. estimations of half-lives and production rates. *Acta Endocrinol.* **121**, 753–758 (1989).

15 Demling, R. H. The Role of Anabolic Hormones for Wound Healing in Catabolic States. *J. Burns Wounds* **4**, e2 (2005).

16 Zhao, Z., Li, Y. & Xie, M.-B. Silk fibroin-based nanoparticles for drug delivery. *Int. J. Mol. Sci.* **16**, 4880–4903, doi:10.3390/ijms16034880 (2015).

17 Cao, Y. & Wang, B. Biodegradation of silk biomaterials. *Int. J. Mol. Sci.* **10**, 1514–1524, doi:10.3390/ijms10041514 (2009).

18 Huang, W., Ling, S., Li, C., Omenetto, F. G. & Kaplan, D. L. Silkworm silk-based materials and devices generated using bio-nanotechnology. *Chem. Soc. Rev.* **47**, 6486–6504, doi:10.1039/c8cs00187a (2018).

19 Inoue, S. *et al.* Silk fibroin of *Bombyx mori* is secreted, assembling a high molecular mass elementary unit consisting of H-chain, L-chain, and P25, with a 6:6:1 molar ratio. *J. Biol. Chem.* **275**, 40517–40528, doi:10.1074/jbc.M006897200 (2000).

20 Shen, Y., Johnson, M. A. & Martin, D. C. Microstructural characterization of *Bombyx mori* silk fibers. *Macromolecules* **31**, 8857–8864, doi:10.1021/ma980281j (1998).

21 Yucel, T., Lovett, M. L. & Kaplan, D. L. Silk-based biomaterials for sustained drug delivery. *J. Control Release* **190**, 381-397, doi:10.1016/j.jconrel.2014.05.059 (2014).

22 Farokhi, M., Mottaghitalab, F., Fatahi, Y., Khademhosseini, A. & Kaplan, D. L. Overview of silk fibroinuse in wound dressings. *Trends Biotechnol.* **36**, 907–922, doi:10.1016/j.tibtech.2018.04.004 (2018).

23 Tran, S. H., Wilson, C. G. & Seib, F. P. A review of the emerging role of silk for the treatment of the eye. *Pharm. Res.* **35**, 1–16, doi:10.1007/s11095-018-2534-y (2018).

24 Padol, A. R. *et al.* Efficacy of the silk protein based biofilms as a novel wound healing agent. *Int. J. Toxicol. Appl. Pharm.* **2**, 31–36 (2012).

25 Shan, Y. H. *et al.* Silk fibroin/gelatin electrospun nanofibrous dressing functionalized with astragaloside IV induces healing and anti-scar effects on burn wound. *Int. J. Pharm.* **479**, 291–301, doi:10.1016/j.ijpharm.2014.12.067 (2015).

26 Gil, E. S., Panilaitis, B., Bellas, E. & Kaplan, D. L. Functionalized silk biomaterials for wound healing. *Adv. Healthc. Mater.* **2**, 206–217, doi:10.1002/adhm.201200192 (2013).

27 Lawrence, B. D., Marchant, J. K., Pindrus, M. A., Omenetto, F. G. & Kaplan, D. L. Silk film biomaterials for cornea tissue engineering. *Biomaterials* **30**, 1299–1308, doi:10.1016/j.biomaterials.2008.11.018 (2009).

28 Gil, E. S. *et al.* Helicoidal multi-lamellar features of RGD-functionalized silk biomaterials for corneal tissue engineering. *Biomaterials* **31**, 8953–8963, doi:10.1016/j.biomaterials.2010.08.017 (2010).

29 Liu, J. *et al.* Silk fibroin as a biomaterial substrate for corneal epithelial cell sheet generation. *Invest. Ophthalmol. Vis. Sci.* **53**, 4130–4138, doi:10.1167/iovs.12-9876 (2012).

30 Kambe, Y., Kojima, K., Tamada, Y., Tomita, N. & Kameda, T. Silk fibroin sponges with cell growth-promoting activity induced by genetically fused basic fibroblast growth factor. *J. Biomed. Mater. Res. A.* **104**, 82–93, doi:10.1002/jbm.a.35543 (2016).

31 Yodmuang, S. *et al.* Silk microfiber–reinforced silk hydrogel composites for functional cartilage tissue repair. *Acta Biomater.* **11**, 27–36, doi:10.1016/j.actbio.2014.09.032 (2015).

32 Min, B. M. *et al.* Electrospinning of silk fibroin nanofibers and its effect on the adhesion and spreading of normal human keratinocytes and fibroblasts in vitro. *Biomaterials* **25**, 1289–1297, doi:10.1016/j.biomaterials.2003.08.045 (2004).

33 Schneider, A., Wang, X. Y., Kaplan, D. L., Garlick, J. A. & Egles, C. Biofunctionalized electrospun silk mats as a topical bioactive dressing for accelerated wound healing. *Acta Biomater.* **5**, 2570–2578, doi:10.1016/j.actbio.2008.12.013 (2009).

34 Wittmer, C. R. *et al.* Multifunctionalized electrospun silk fibers promote axon regeneration in central nervous system. *Adv. Funct. Mater.* **21**, 4202, doi:10.1002/adfm.201190103 (2011).

35 Chopra, S. & Gulrajanii, M. L. Comparative evaluation of the various methods of degumming silk. *Indian J. of Fibre Text. Res.* **19**, 76–83 (1994).

36 Khan, M. R. *et al.* Physical properties and dyeability of silk fibers degummed with citric acid. *Bioresour. Technol.* **101**, 8439–8445, doi:10.1016/j.biortech.2010.05.100 (2010).

37 Cao, T. T., Wang, Y. J. & Zhang, Y. Q. Effect of strongly alkaline electrolyzed water on silk degumming and the physical properties of the fibroin fiber. *PLoS One* **8**, e65654, doi:10.1371/journal.pone.0065654 (2013).

38 Aramwit, P., Damrongsakkul, S., Kanokpanont, S. & Srichana, T. Properties and antityrosinase activity of sericin from various extraction methods. *Biotechnol. Appl. Biochem.* **55**, 91–98, doi:10.1042/ba20090186 (2010).

39 Kunz, R. I., Brancalhao, R. M., Ribeiro, L. F. & Natali, M. R. Silkworm sericin: properties and biomedical applications. *Biomed. Res. Int.* **2016**, 8175701, doi:10.1155/2016/8175701 (2016).

40 Ohlsson, C. *et al.* The role of liver-derived insulin-like growth factor-I. *Endocr. Rev.* **30**, 494–535, doi:10.1210/er.2009-0010 (2009).

41 Laron, Z. Insulin-like growth factor 1 (IGF-1): a growth hormone. *Mol. Path.* **54**, 311–316 (2001).

42 Bright, G. M. Recombinant IGF-I: past, present and future. *Growth Horm. IGF Res.* **28**, 62–65, doi:10.1016/j.ghir.2016.01.002 (2016).

43 Delafontaine, P., Song, Y. H. & Li, Y. Expression, regulation, and function of IGF-1, IGF-1R, and IGF-1 binding proteins in blood vessels. *Arterioscler. Thromb. Vasc. Biol.* **24**, 435–444, doi:10.1161/01.ATV.0000105902.89459.09 (2004).

44 Ando, Y. & Jensen, P. J. Epidermal growth factor and insulin-like growth factor I enhance keratinocyte migration. *J. Invest. Dermatol.* **100**, 633–639, doi:10.1111/1523-1747.ep12472297 (1993).

45 Haase, I., Evans, R., Pofahl, R. & Watt, F. M. Regulation of keratinocyte shape, migration and wound epithelialization by IGF-1- and EGF-dependent signalling pathways. *J. Cell Sci.* **116**, 3227–3238, doi:10.1242/jcs.00610 (2003).

46 Sadagurski, M. *et al.* Insulin-like growth factor 1 receptor signaling regulates skin development and inhibits skin keratinocyte differentiation. *Mol. Cell. Biol.* **26**, 2675–2687, doi:10.1128/MCB.26.7.2675-2687.2006 (2006).

47 Wang, J., Zhou, J. & Bondy, C. A. Igf1 promotes longitudinal bone growth by insulin-like actions augmenting chondrocyte hypertrophy. *The FASEB Journal* **13**, 1985–1990 (1999).

48 Achar, R. A. N., Silval, T. C., Achar, E., Martines, R. B. & Machado, J. L. M. Use of insulin-like growth factor in the healing of open wounds in diabetic and non-diabetic rats. *Acta Cir. Bras.* **29**, 125–131 (2014).

Figures

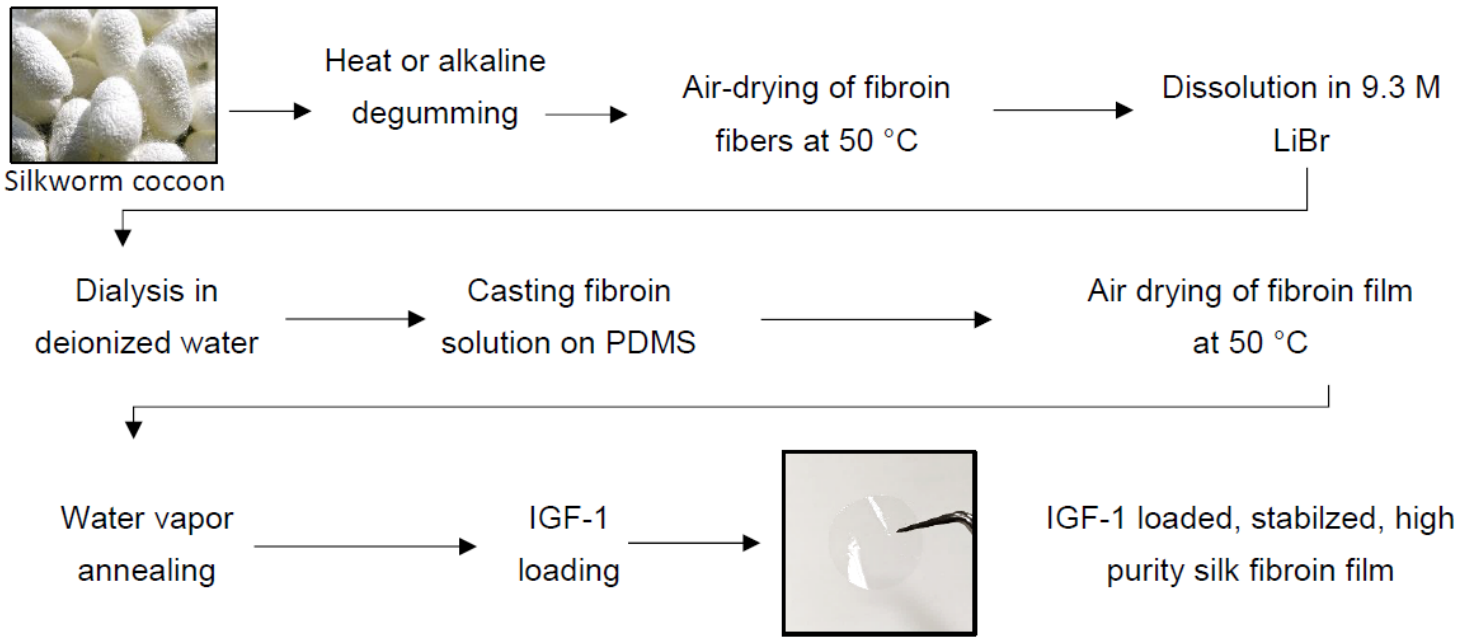

Figure 1

Preparation of insulin-like growth factor 1 (IGF-1)-loaded silk fibroin films (SF-film). Scheme for stepwise synthesis of IGF-1-loaded SF-film. PDMS, polydimethylsiloxane.

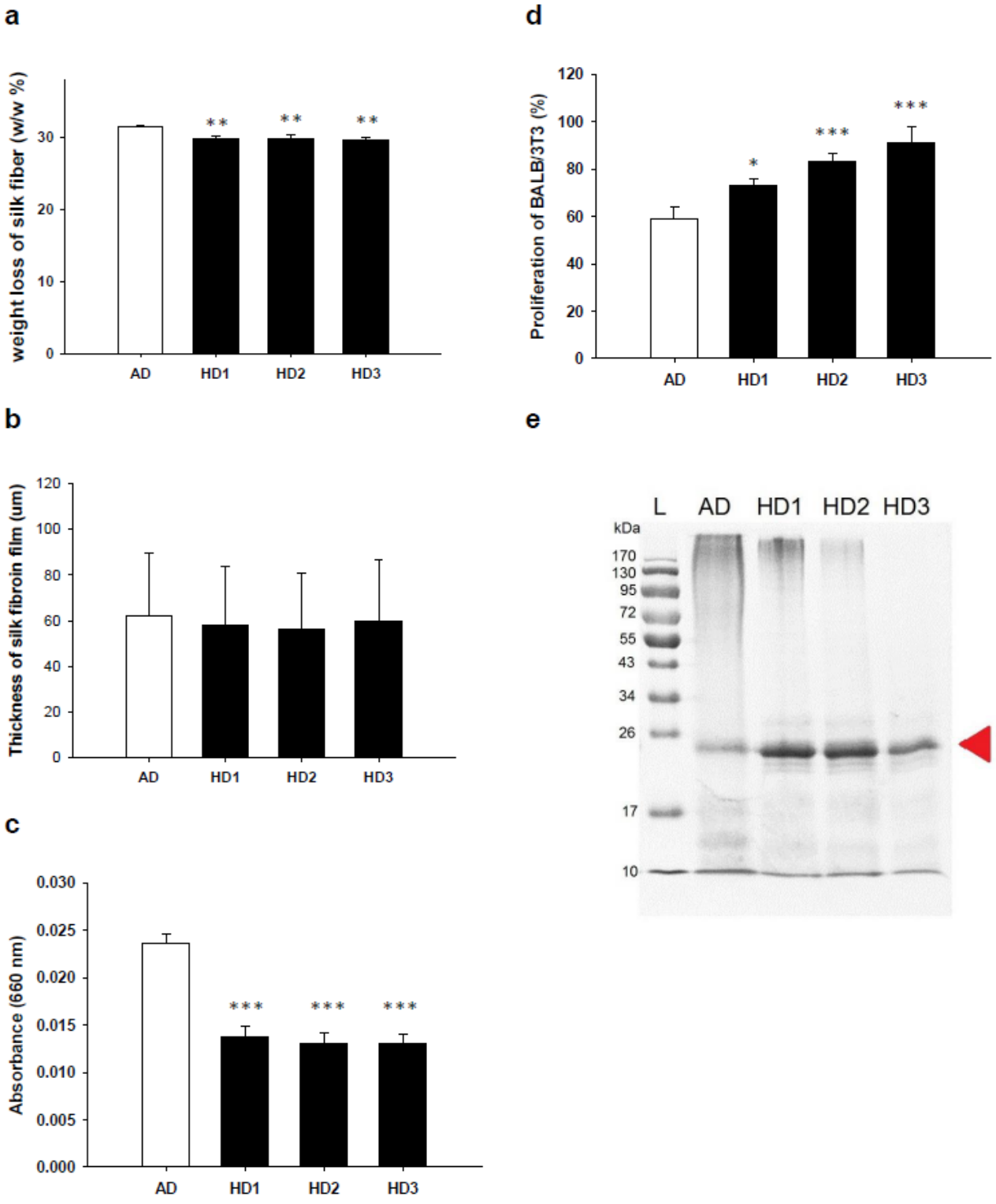

Figure 2

Comparison of silk fibroin purified from alkaline and heat degumming procedures. Comparison of weight loss (a) and thickness (b) of silk fibers after alkaline degumming (AD) and heat degumming for 1, 2, and 3 h (HD1, HD2, and HD3). Transparency (c) of the fibroin films prepared by AD and HD1–3 procedures. Viability of BALB/3T3 fibroblasts (d) grown on these SF-films, and SDS–PAGE of the fibroin prepared by AD and HD1–3 procedures (e), L indicates the pre-stained protein ladder. Significant differences between

AD and HD were determined by Dunnett's multiple comparison post hoc test. *p < 0.05, and **p < 0.01, and *** p < 0.001; n = 4; mean ± SEM.

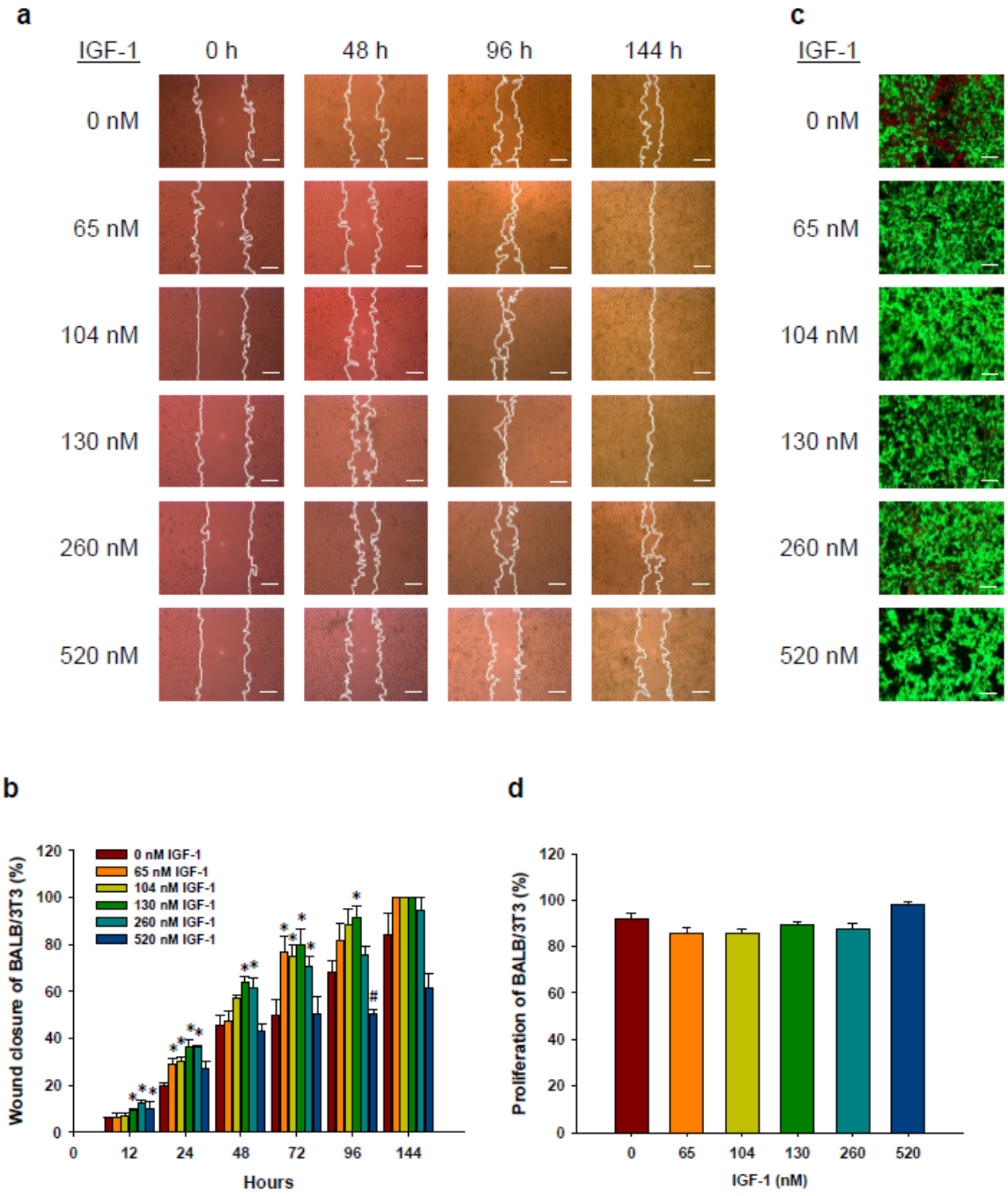

Figure 3

Effects of IGF-1 on BALB/3T3 fibroblast migration, cytotoxicity, wound healing, and proliferation. (a) Bright-field images of BALB/3T3 monolayer wound healing in the presence of different amounts of IGF-1 at different times. Scale bars = 200 μm. (b) Improvement of BALB/3T3 cell wound closure by IGF-1. (c)

Cytotoxicity of IGF-1 toward BALB/3T3 cells. Cells were treated with different concentrations of IGF-1, stained with LIVE/DEAD stain and examined under a fluorescence microscope. Scale bars = 200 μm. (d) Cell proliferation in the presence of different amounts of IGF-1. Significant differences between untreated (control) and IGF-1-treated cells were determined by Dunnett's multiple comparison post hoc test. *p < 0.05 and #p < 0.001; n = 4; mean ± SEM.

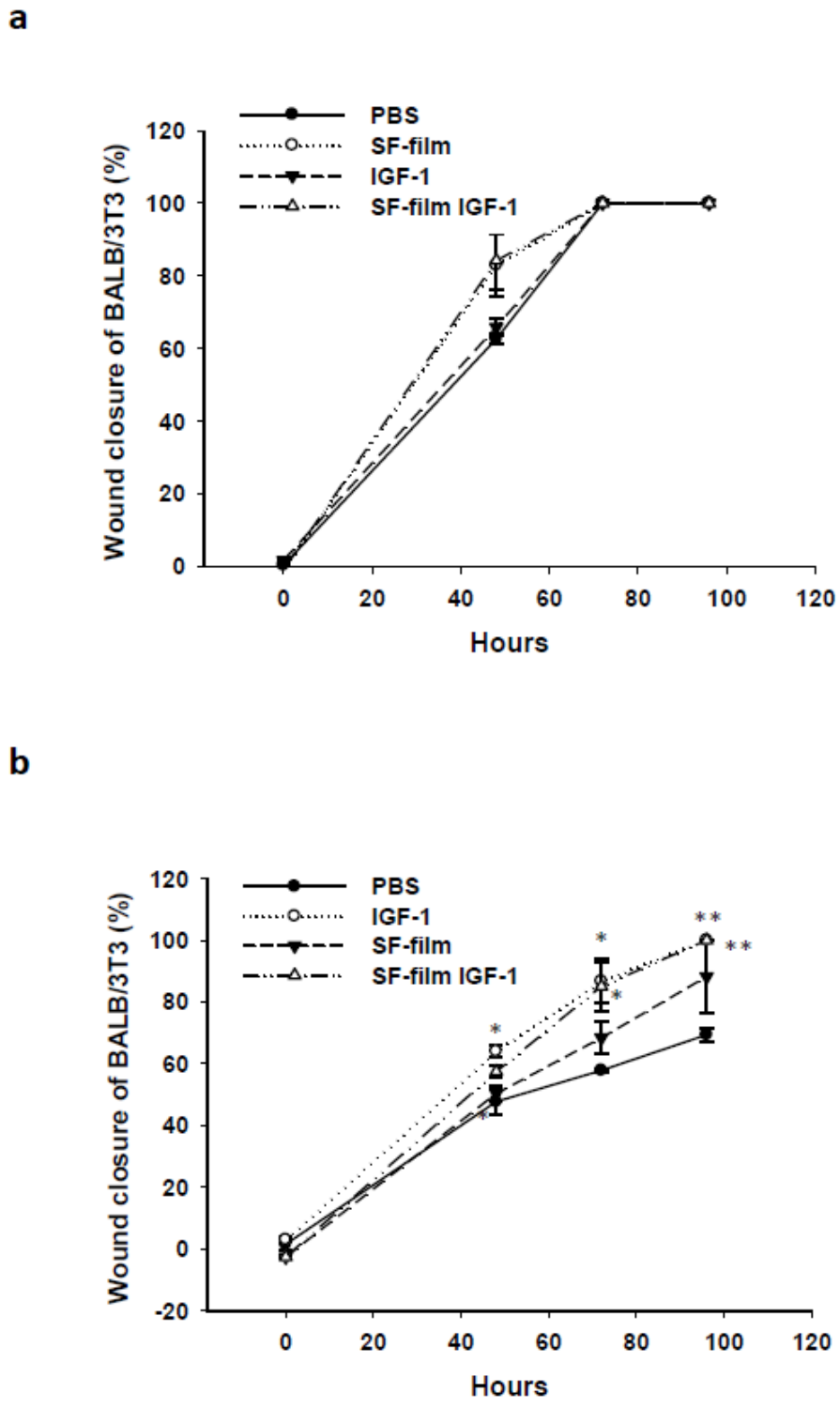

Figure 4

Migration of BALB/3T3 fibroblasts in response to IGF-1, SF-film, and IGF-1-loaded SF-film (SF-film-IGF-1) treatments. Quantification of cell wound closure after IGF-1, SF-film, or IGF-1-loaded SF-film treatment in regular medium (a) or hyperglycemic medium (b). Significant differences between the PBS and treatment groups were determined by Dunnett's multiple comparison post hoc test. *p < 0.05 and **p < 0.01; n = 4; mean ± SEM.

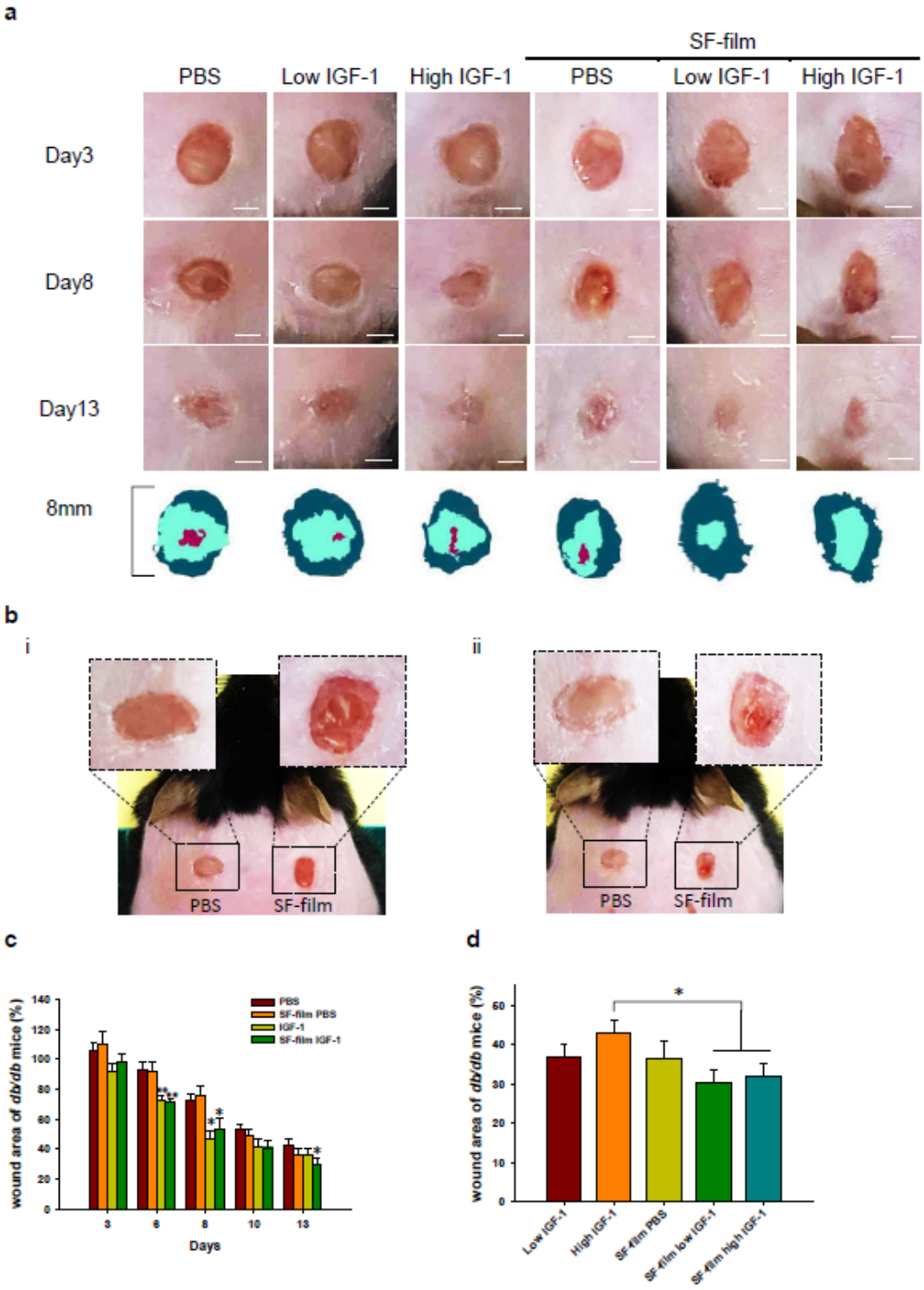

Figure 5

Analysis of diabetic wound healing after different treatments. (a) Images of the wound area from day 0 to 13 post-wounding; scale = 5 mm. Wound closure boundaries at day 0 (dark green) and 13 (light green) and unhealed tissue at day 13 (red) are overlaid at the bottom. (b) Images of 8-mm full-thickness dorsal wounds in db/db mice five (i) and eight (ii) days post-wounding. The wounds were treated with PBS (left) and PBS/SF-film (right). (c) Quantification of wound closure upon different treatments. Significant differences between PBS and other treatments were determined by Dunnett's multiple comparison post hoc test. *$p < 0.05$, and **$p < 0.01$; $n = 5$; ±SEM. (d) Quantification of the wound area at day 13 post-wounding after different treatments. Significant differences between high IGF-1 and other treatments were determined by Dunnett's multiple comparison post hoc test. *$p < 0.05$ and **$p < 0.01$; $n = 5$; mean ± SEM.

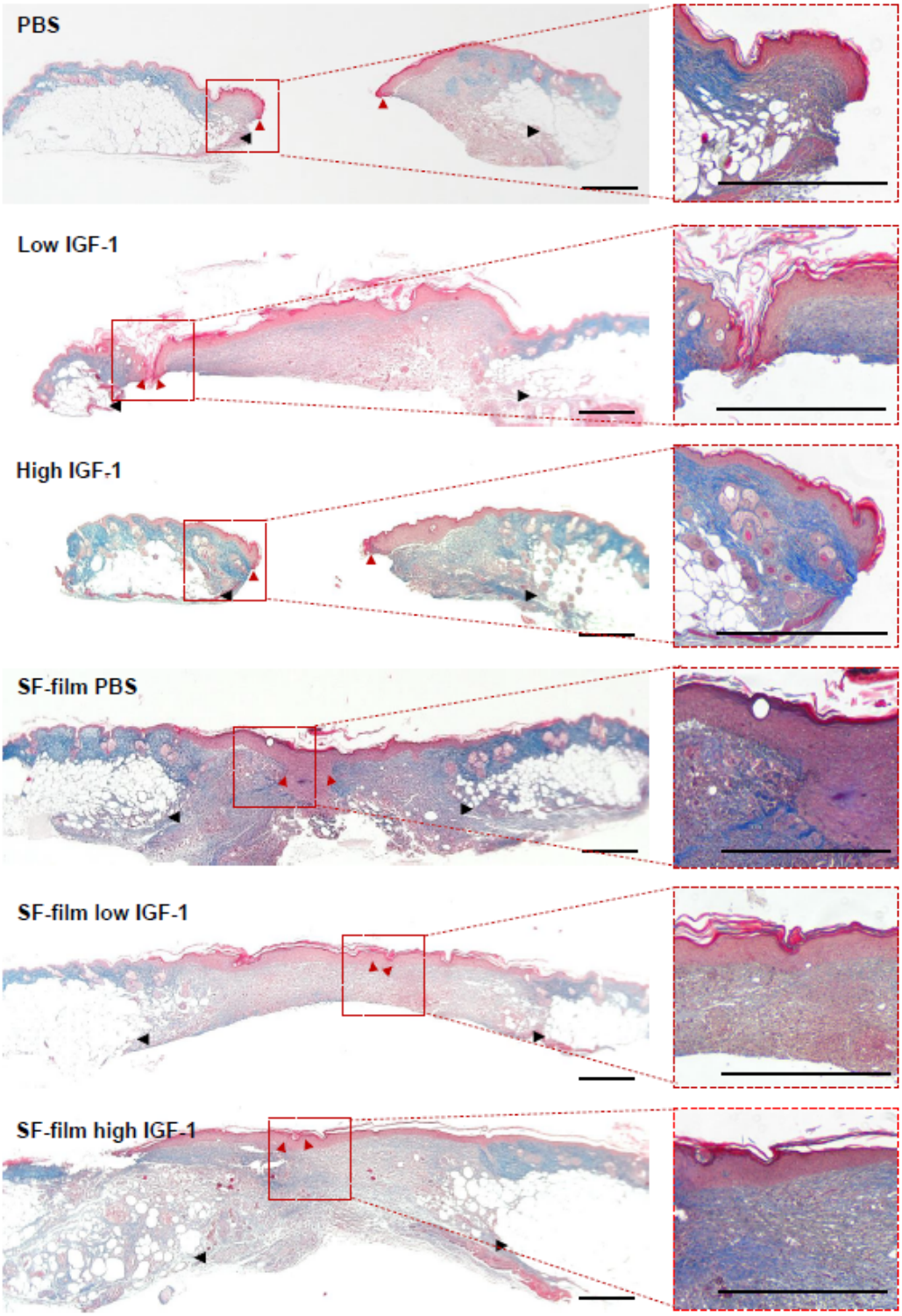

Figure 6

Masson's trichrome staining of the wound area after different treatments. Tissues at day 13 post-wounding were histologically analyzed. Wound edge, black arrowheads; tips of the epithelial tongue, red arrowheads; scale = 500 μm.

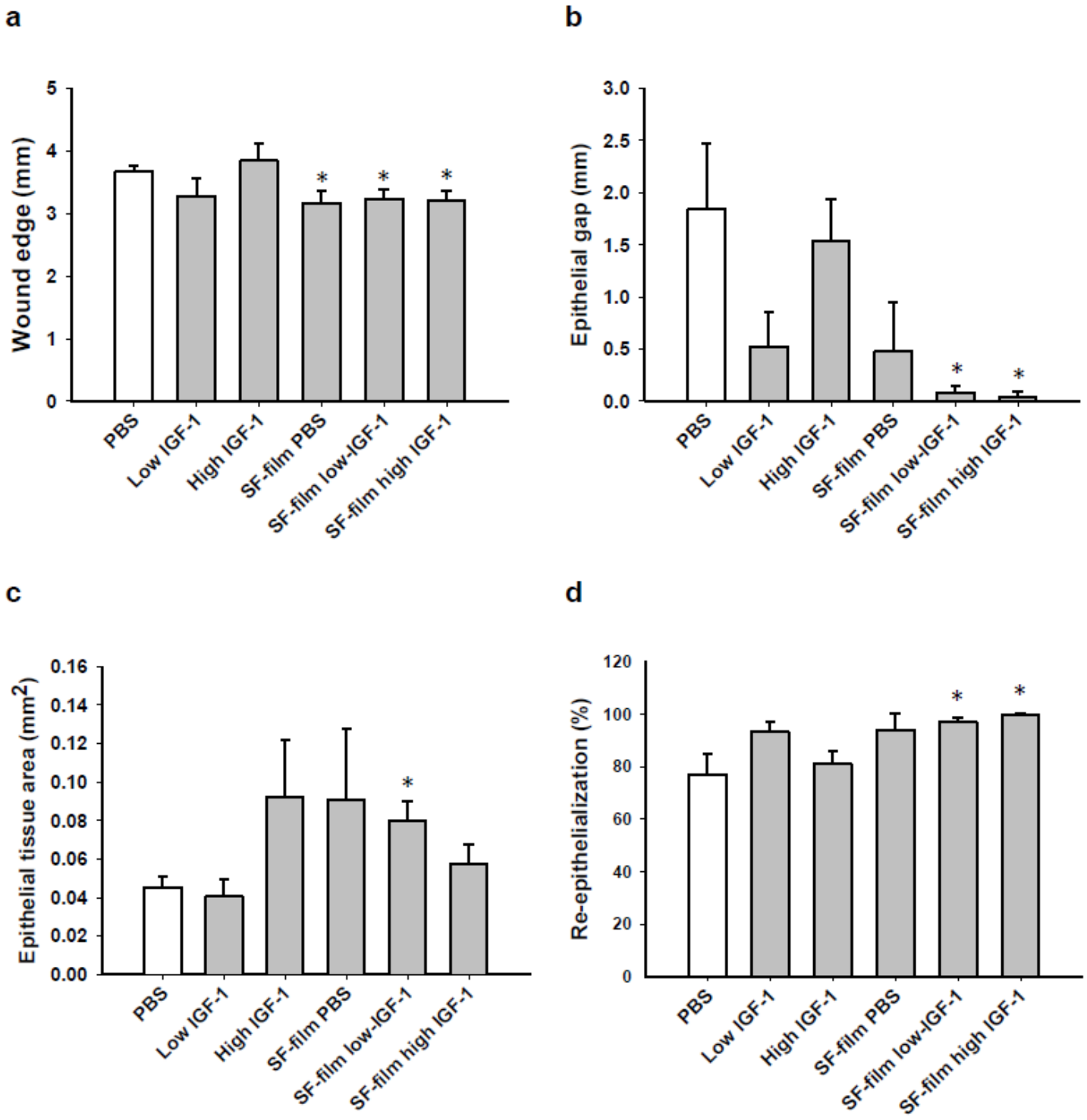

Figure 7

Effects of IGF-1, SF film, and IGF-1-loaded SF-film (SF-film-IGF-1) on tissue regeneration in diabetic wounds. Tissues at day 13 post-wounding were histologically analyzed. Quantification of (a) wound edge distance, (b) epithelial gap, (c) epithelial tissue area, and (d) re-epithelialization after wound healing at day 13 post-wounding is shown. Significant differences between PBS and each of the treatments were determined by Dunnett's multiple comparison post hoc test. *$p < 0.05$; $n = 5$; mean ± SEM.

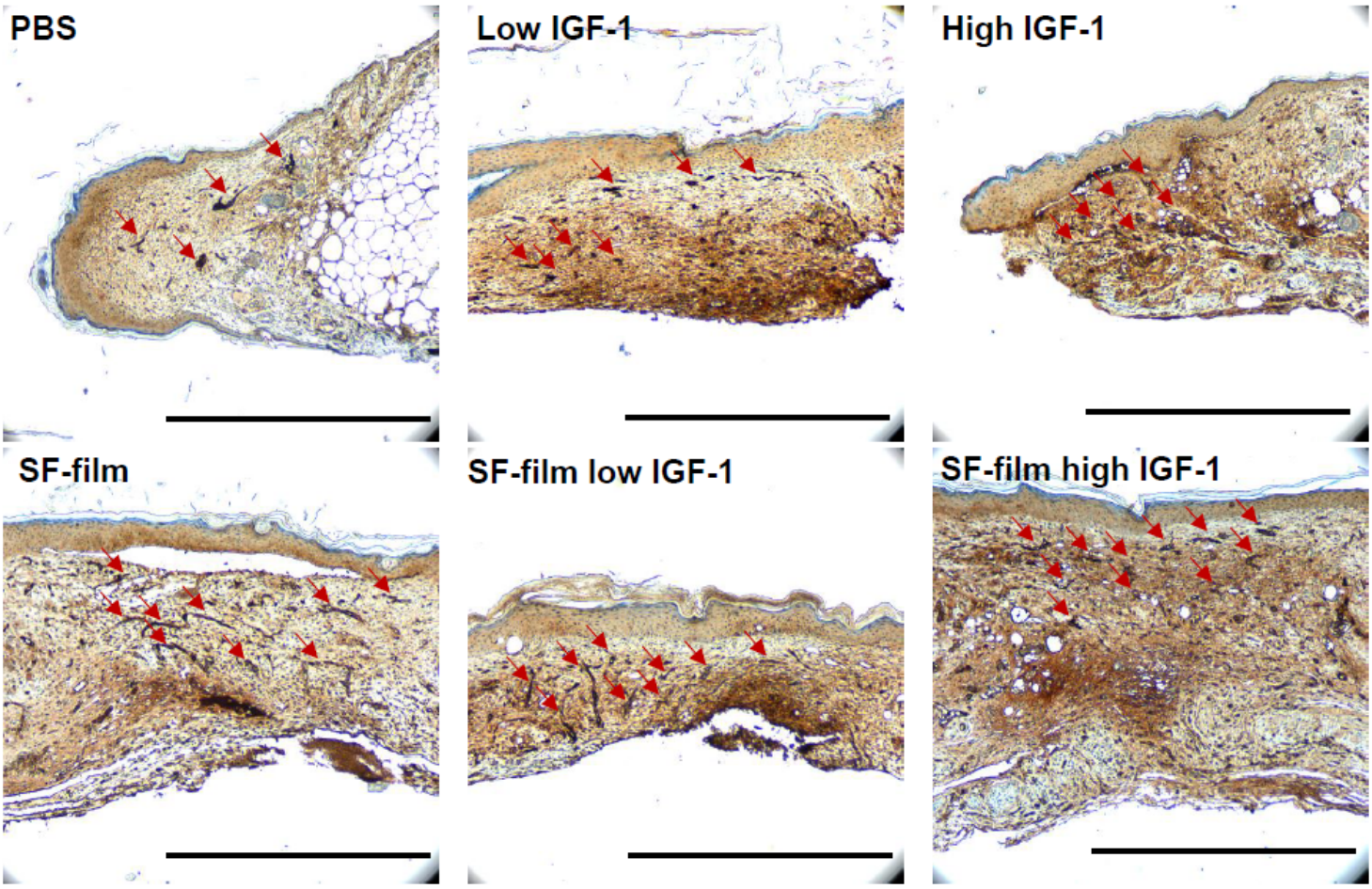

Figure 8

Effects of IGF-1, SF film, and IGF-1-loaded SF-film (SF-film-IGF-1) on blood vessel growth in diabetic wounds. Blood vessel density in diabetic wounds after different treatments were determined immunohistologically by staining the tissue sections blotted with an anti-human CD31 antibody. The presence of blood vessels is indicated by red arrows. Scale bars = 500 μm.

Supplementary Files

This is a list of supplementary files associated with this preprint. Click to download.

- 59782SupplementaryFigures20210408.docx